OAK RIDGE NATIONAL LABORATORY LIBRARIES

3 4456 0551465 4

ORNL/TM-6456

Ultrasonic Flaw Detection and Characterization in Structural Materials by Spectral Analysis

L. Adler
K. V. Cook
W. A. Simpson
D. K. Lewis
D. W. Fitting

[redacted]

OAK RIDGE NATIONAL LABORATORY
CENTRAL RESEARCH LIBRARY
CIRCULATION SECTION
4500N ROOM 175
LIBRARY LOAN COPY
DO NOT TRANSFER TO ANOTHER PERSON
If you wish someone else to see this report, send in name with report and the library will arrange a loan.

OAK RIDGE NATIONAL LABORATORY
OPERATED BY UNION CARBIDE CORPORATION - FOR THE DEPARTMENT OF ENERGY

Printed in the United States of America. Available from
the Department of Energy,
Technical Information Center
P.O. Box 62, Oak Ridge, Tennessee 37830
Price: Printed Copy $4.50; Microfiche $3.00

This report was prepared as an account of work sponsored by an agency of the United States Government. Neither the United States Government nor any agency thereof, nor any of their employees, contractors, subcontractors, or their employees, makes any warranty, express or implied, nor assumes any legal liability or responsibility for any third party's use or the results of such use of any information, apparatus, product or process disclosed in this report, nor represents that its use by such third party would not infringe privately owned rights.

ORNL/TM-6456
Distribution
Category
UC-79b, -h, -k

Contract No. W-7405-eng-26

METALS AND CERAMICS DIVISION

ULTRASONIC FLAW DETECTION AND CHARACTERIZATION IN STRUCTURAL MATERIALS BY SPECTRAL ANALYSIS

L. Adler, K. V. Cook, W. A. Simpson, D. K. Lewis, and D. W. Fitting

Date Published: October 1978

NOTICE This document contains information of a preliminary nature. It is subject to revision or correction and therefore does not represent a final report.

OAK RIDGE NATIONAL LABORATORY
Oak Ridge, Tennessee 37830
operated by
UNION CARBIDE CORPORATION
for the
DEPARTMENT OF ENERGY

OAK RIDGE NATIONAL LABORATORY LIBRARIES
3 4456 0551465 4

CONTENTS

ABSTRACT 1

INTRODUCTION 1

THEORY 2

Ultrasonic Wave Propagation in Anisotropic Solids with Orthotropic Symmetry 2

Diffraction of Ultrasonic Waves at Flaws 5

EXPERIMENTAL SYSTEMS 7

Measurements of Ultrasonic Velocities as a Function of Orientation in Structured Materials 7

Data Analysis 9

Results 9

APPARATUS FOR FREQUENCY ANALYSIS 14

For Analog Data 14

Modified Experimental System and Signal Processing 14

RESULTS 18

ACKNOWLEDGMENTS 22

REFERENCES 22

ULTRASONIC FLAW DETECTION AND CHARACTERIZATION IN STRUCTURAL MATERIALS BY SPECTRAL ANALYSIS*

L. Adler, K. V. Cook, W. A. Simpson, D. K. Lewis,† and D. W. Fitting

ABSTRACT

A method of quantitatively determining size and location of simulated flaws in anisotropic materials such as stainless steel welds is described. Previous work demonstrated that spectral analysis of a broad-band ultrasonic pulse scattered from a defect can be used to determine its size and orientation in isotropic materials if the velocity of sound in the material is known. In an anisotropic structural material — stainless steel weld, centrifugally cast pipe — the velocity of sound — both shear and longitudinal — depends on the sound's direction. When anisotropy is not taken into account, defect location and size are frequently misjudged. The effect of this structural variation in materials must be considered to obtain the correct size and location of defects by frequency analysis. A theoretical calculation, including anisotropy, of the scattered field from defects is also presented.

INTRODUCTION

An important application of nondestructive evaluation (NDE) is the detection of cracks or inclusions in metallic components and the determination of their location. In addition to defect location, defect characterization is becoming increasingly important in modern NDE. Defect characterization refers to the determination of size, shape, orientation, and composition of the defect. In conventional ultrasonic testing the beam reflected from a defect is observed and the location of the defect is determined from the time the ultrasonic pulse takes to travel to and from the defect. The size of the defect, on the other hand, is estimated by measuring the amplitude of the reflected ultrasonic wave.

---

*Work performed under DOE/RRT 189a OH061, "Nondestructive Testing."
†Graduate student from the University of Tennessee.

The measurement of the sound wave's travel time accurately locates the defect. Amplitude measurements, however, can result in size estimations in error by a factor of as much as 5 to 10 if the orientation of the defect is not normal to the incident beam.[1] To overcome this difficulty ultrasonic spectral analysis has been developed to make defect size determinations to supplement those based on amplitude measurements.[3–7]

Spectral analysis, which uses frequency distribution of the scattered amplitude to characterize flaws, has been successfully applied in aluminum and in carbon steel. Conventional ultrasonic techniques detect and characterize flaws poorly in austenitic steels with welded or cast structures. Very often ultrasonic time measurements do not locate the defect properly when the weld itself is sectioned. The reason for this discrepancy may be explained by a recent study[2] of austenitic steel, which showed mechanical anisotropy caused by preferred local orientation of elongated subgrains. As a result, the velocity of propagation for both shear and longitudinal waves will depend on the direction of the sound waves. The purpose of this paper is to show: (1) how ultrasonics will enable us to clearly describe this anisotropic behavior and (2) how the information about anisotropy is used to locate and characterize defects in anisotropic materials.

THEORY

Ultrasonic Wave Propagation in Anisotropic Solids with Orthotropic Symmetry

The apparent symmetry in the macrostructure of an austenitic stainless steel weld suggested[2] orthotropic symmetry for the stress-strain relationship. The general relation of stress to strain in matrix notation is

$$\{\sigma\} = [C]\{\varepsilon\} \ , \tag{1}$$

where $\{\theta\}$ is the stress matrix, $\{\varepsilon\}$ is the strain matrix, and $[C]$ is the elastic stiffness matrix. For a material with orthotropic symmetry there are nine independent terms in $[C]$:

$$[C] = \begin{bmatrix} C_{11} & C_{12} & C_{13} & 0 & 0 & 0 \\ C_{12} & C_{22} & C_{23} & 0 & 0 & 0 \\ C_{13} & C_{23} & C_{33} & 0 & 0 & 0 \\ 0 & 0 & 0 & C_{44} & 0 & 0 \\ 0 & 0 & 0 & 0 & C_{55} & 0 \\ 0 & 0 & 0 & 0 & 0 & C_{66} \end{bmatrix} \tag{2}$$

Inversion of Eq. 2 yields in matrix notation

$$\{\varepsilon\} = [C]^{-1}\{\sigma\} = [s]\{\sigma\} \ , \tag{3}$$

where $[s]$ is the elastic compliance matrix.
The relationship between the elastic stiffness constants and the velocity of the ultrasonic wave is expressed by the Christoffel relation:

$$\begin{vmatrix} \lambda_{11} - \rho V^2 & \lambda_{12} & \lambda_{13} \\ \lambda_{12} & \lambda_{22} - \rho V^2 & \lambda_{23} \\ \lambda_{13} & \lambda_{23} & \lambda_{33} - \rho V^2 \end{vmatrix} = 0 \ , \tag{4}$$

where, for a material with orthotropic symmetry

$$\begin{aligned} \lambda_{11} &= \ell^2 C_{11} + m^2 C_{66} + n^2 C_{55} \\ \lambda_{12} &= \ell m (C_{12} + C_{66}) \\ \lambda_{13} &= n\ell (C_{13} + C_{55}) \\ \lambda_{22} &= \ell^2 C_{66} + m^2 C_{22} + n^2 C_{44} \\ \lambda_{23} &= mn (C_{44} + C_{23}) \\ \lambda_{33} &= \ell^2 C_{55} + m^2 C_{44} + n^2 C_{33} \end{aligned} \tag{5}$$

where l, m and n are direction cosines of the propagation direction and ρ is the density of the material. A coordinate system attached to the weld is defined in Fig. 1. The elements of the elastic stiffness matrix are calculated by measuring sound velocity in a number of specified directions and by applying the following relation.

Table 1. Relationships Between Elastic Stiffness and Ultrasonic Propagation Velocity

Propagation Direction	Elastic Stiffness Relations[a]
1 axis	$C_{11} = \rho V_{11}^2,\ C_{66} = \rho V_{12}^2,\ C_{55} = \rho V_{13}^2$
2 axis	$C_{22} = \rho V_{22}^2,\ C_{66} = \rho V_{21}^2,\ C_{44} = \rho V_{23}^2$
3 axis	$C_{33} = \rho V_{33}^2,\ C_{55} = \rho V_{31}^2,\ C_{44} = \rho V_{32}^2$
1′ axis (Rotation around 3)	$C_{12} = l^{-1}m^{-1}[(l^2C_{11} + m^2C_{66} - \rho V_{11}'^2)(l^2C_{66} + m^2C_{22} - \rho V_{11}'^2)]^{1/2} - C_{66}$
2′ axis (Rotation around 1)	$C_{23} = m^{-1}n^{-1}[(m^2C_{22} + n^2C_{44} - \rho V_{22}'^2)(m^2C_{44} + n^2C_{33} - \rho V_{22}'^2)]^{1/2} - C_{44}$
3′ axis (Rotation around 2)	$C_{13} = n^{-1}l^{-1}[(n^2C_{11} + l^2C_{55} - \rho V_{33}'^2)(n^2C_{55} + l^2C_{33} - \rho V_{33}'^2)]^{1/2} - C_{55}$

[a]The first subscript on V indicates the direction of propagation and the second subscript indicates the polarization; e.g., V_{31} represents shear velocity propagating in the 3-direction and polarized along the 1-direction. Once the elastic constants are calculated from the relations above, the last three equations can be solved to calculate the variations of the velocities as a function of orientation.

ORNL-DWG 75-13166R

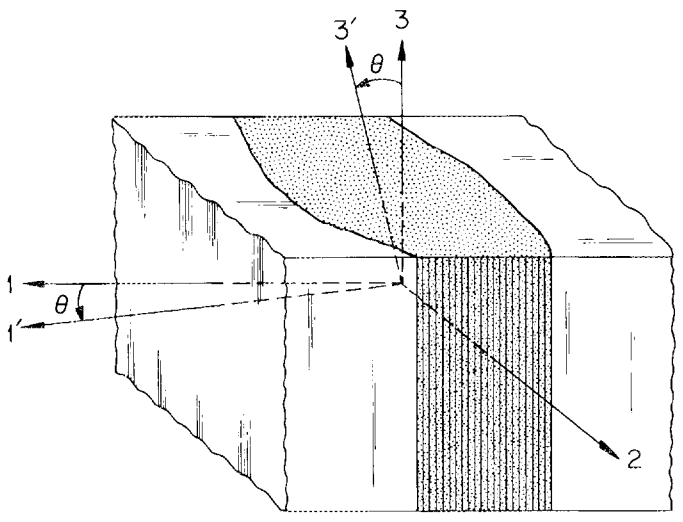

Fig. 1. Reference Coordinate Axes and Illustration of an Electroslag Weld with the Idealization of all Solidification Directions as Parallel.

For some applications "engineering" constants may be more convenient than the components of the $[s]$ or $[c]$ matrix. The engineering constants are most conveniently derived from the compliance matrix, where

$$
\begin{aligned}
E_1 &= 1/S_{11} \\
E_2 &= 1/S_{22} \\
E_3 &= 1/S_{33} \\
G_{32} &= 1/S_{44} = C_{44} \\
G_{31} &= 1/S_{55} = C_{55} \\
G_{21} &= 1/S_{66} = C_{66} \\
\nu_{32} &= -S_{23}/S_{22} \\
\nu_{31} &= -S_{13}/S_{11} \\
\nu_{21} &= -S_{12}/S_{11}
\end{aligned}
\tag{6}
$$

where E_i represents the modulus of elasticity in direction i; G_{ij} represents the shear modulus in the ij plane; and ν_{ij} represents the ratio of the strain in the j-direction to the strain in the i-direction.

Diffraction of Ultrasonic Waves at Flaws

In order to characterize unknown flaws in materials, one needs to have previous knowledge of wave interaction with known, well-defined flaws. Then with this knowledge one can attempt the inverse problem; namely, to determine the size, shape, and orientation of a flaw by analyzing the scattered ultrasonic waves. The scattering mechanism for defects large compared with the wave length is called <u>diffraction</u>. A geometrical theory of diffraction developed for electromagnetic waves[8] and adopted for ultrasonic waves[7] relates the intensity distribution

of the diffracted waves in frequency space to the geometric characteristics of the flaw. For a circular crack with radius a, the amplitude of the scattered ultrasonic wave at a point in the far field is of the form

$$U \equiv A(k) \left[\frac{2}{\sqrt{k}(\sin\theta + \sin\alpha)} \right] \left\{ \frac{\sin^2[ka(\sin\theta + \sin\alpha) - \frac{\pi}{4}]}{\sin^2\left(\frac{\theta + \alpha}{2}\right)} + \frac{\cos^2[ka(\sin\theta + \sin\alpha) - \frac{\pi}{4}]}{\cos^2\left(\frac{\theta - \alpha}{2}\right)} \right\}^{\frac{1}{2}} , \tag{7}$$

where α is the incident angle, θ is the scattered angle and $A(k)$ is the the amplitude distribution of the incident wave. For the case of normal incidence ($\alpha = 0$) or pulse-echo technique ($\alpha = \theta$), Eq. (7) becomes simpler.

The diffracted amplitude for scattered shear and scattered longitudinal waves from a circular defect in steel (for a = 6 mm), calculated by using Eq. (7), is shown in Fig. 2. The scattered angle varies from 30 to 60° and the frequency ranges from 2 to 6 MHz. Notice the characteristic amplitude variation with frequency. The so-called interference model[1] developed earlier to determine size of defects uses the frequency spacing Δf of the amplitude maxima. The radius of the circular crack is

$$a = \frac{V}{\Delta f \sin\theta} . \tag{8}$$

In the case of an anisotropic material, V is a function of direction (θ). In order to calculate scattered amplitude (V) from Eq. (7), as well as to determine the size (a) of the crack, the functional relationship between V and θ must first be determined.

ORNL-DWG 78-10005

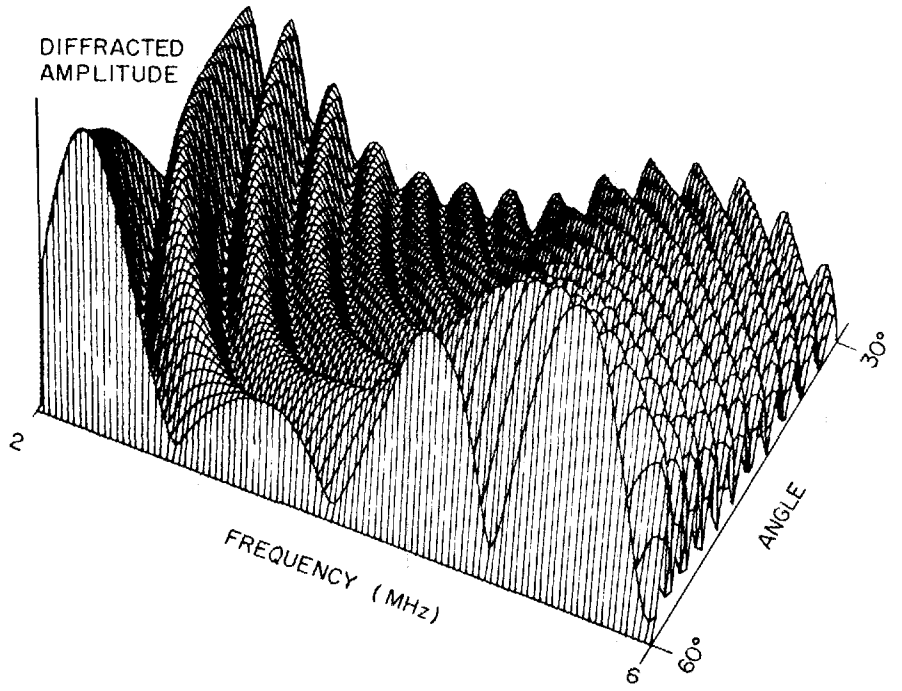

Fig. 2. Calculated Diffracted Amplitude from a Circular Defect (6-mm radius).

EXPERIMENTAL SYSTEMS

Measurements of Ultrasonic Velocities as a Function of Orientation in Structured Materials

An apparatus developed to measure variation of velocities with direction in structured materials is illustrated in Fig. 3. A cylindrical sample mounted on a goniometer is slowly rotated about its axis. Ultrasound is transmitted through the sample on a fixed-distance path from transmitter to receiver; both transmitting and receiving transducers are 5-MHz (center-frequency) units. The signal transmitted through the sample is displayed on an oscilloscope and the variation in velocity is measured by noting the time shift of the ultrasonic waveform. An aluminum reference cylinder helps to align the system. This technique can detect velocity variations of about 1%.

Three cylindrical samples and a cubical sample (Fig. 4) are machined from the weld. The three cylinders are selected such that

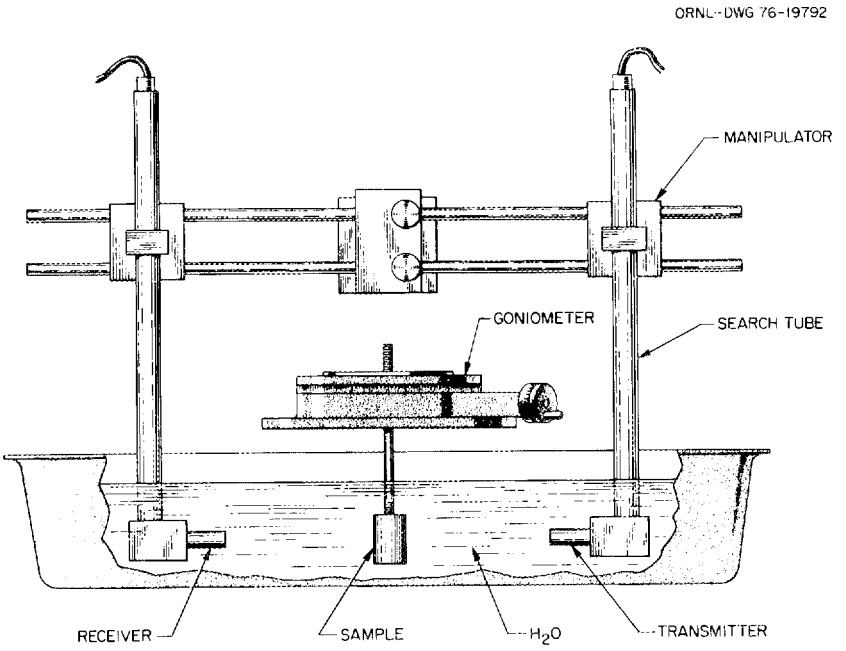

Fig. 3. Apparatus to Measure Longitudinal Velocity Variations in a Cylindrical Sample.

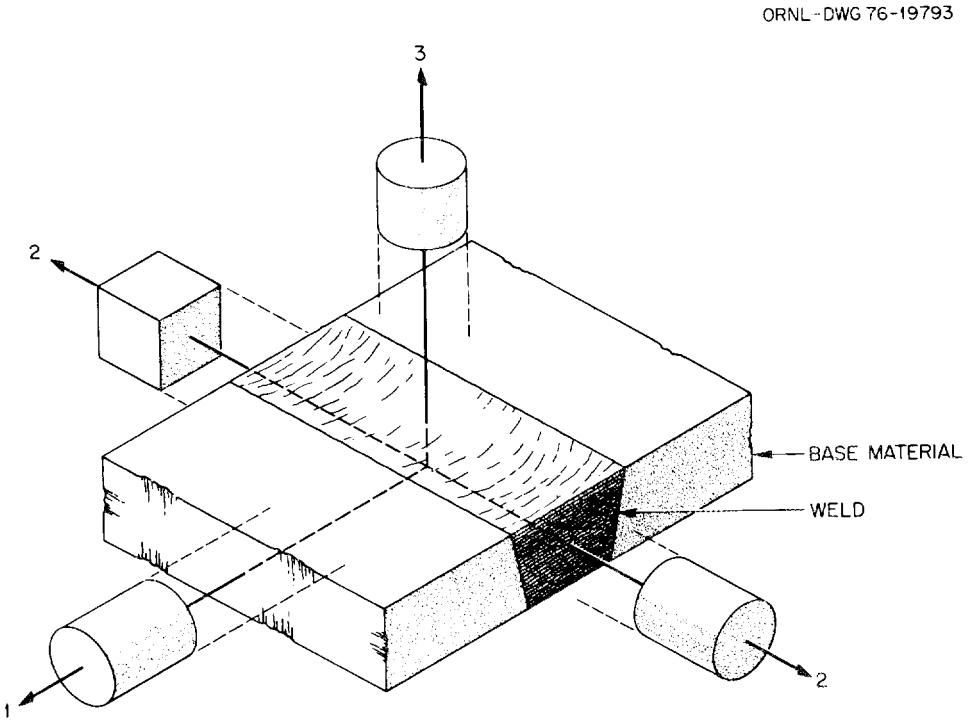

Fig. 4. Sample Selection from a Section of Weld for Ultrasonic Studies.

their axes lie along the coordinate axes. The cylinders are used to measure the velocity changes with orientation. Rotating each sample about its axis yields continuous data on longitudinal velocity as a function of orientation in the three orthogonal planes. For example, rotating the sample about its 2-axis gives not only V_{11} and V_{33} but also V'_{33} (see Table 1), which is required to calculate the elastic constants. The cube's contact longitudinal- and shear-wave velocities must be measured to convert the relative velocities determined from the cylindrical samples to absolute velocities.

Data Analysis

A computer program in FORTRAN was used to calculate important parameters. This program, an interactive one, accepts longitudinal and shear velocity data for the sample. Program output includes (1) the elements of the elastic stiffness and compliance matrices and (2) theoretical longitudinal- and shear-wave velocities at 5° intervals in three orthogonal planes. The computer program was written to follow the method of calculation outlined in Section II.

Results

Two weld materials were available: (1) an electroslag single-pass weld of type 308 stainless steel and (2) an Inconel 82 multipass weld (47 passes). Plots of theoretical and experimental velocity data for these two welds are given in Figs. 5 and 6. Figure 5 shows only the planes demonstrating anisotropy. The longitudinal data were obtained by through transmission directly across the diameter of the sample. Shear-wave data were from the cubical specimen. The solid curve is theoretical and is obtained by solving the last three equations of Table 1 for the primed velocities. Dots denote experimental results.

Experimental data are also presented in Figs. 7 and 8 for the variation of attenuation with orientation for the two welds. Again, plots for the single-pass weld do not include the plane of isotropy.

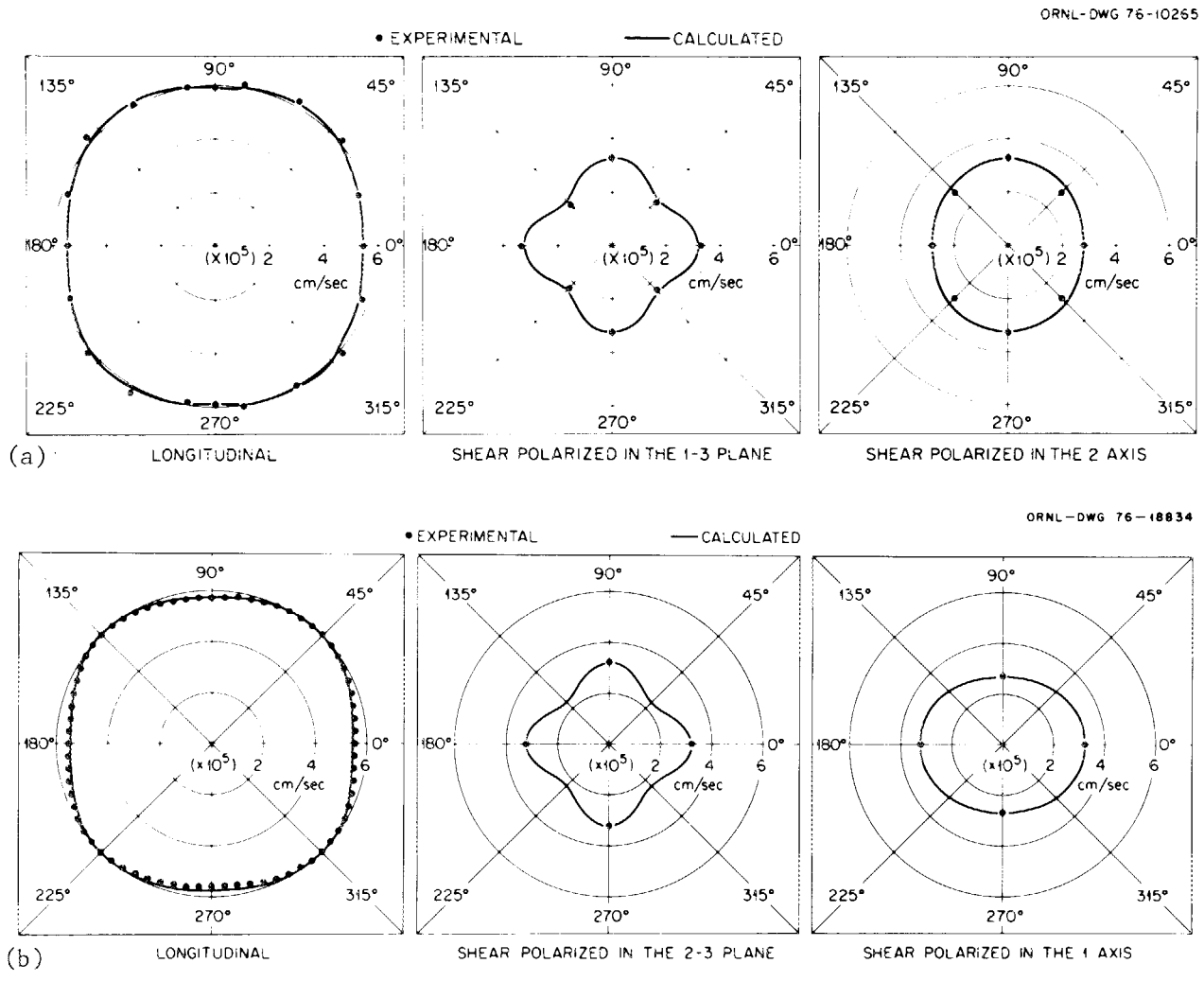

Fig. 5. Anisotropic Variation of Velocity in Type 308 Stainless Steel Weld Metal. The solid curves are calculated from the Christoffel relation for the assumed orthotropic symmetry. Points are experimental. (a) In the 1—3 plane. (b) In the 2—3 plane.

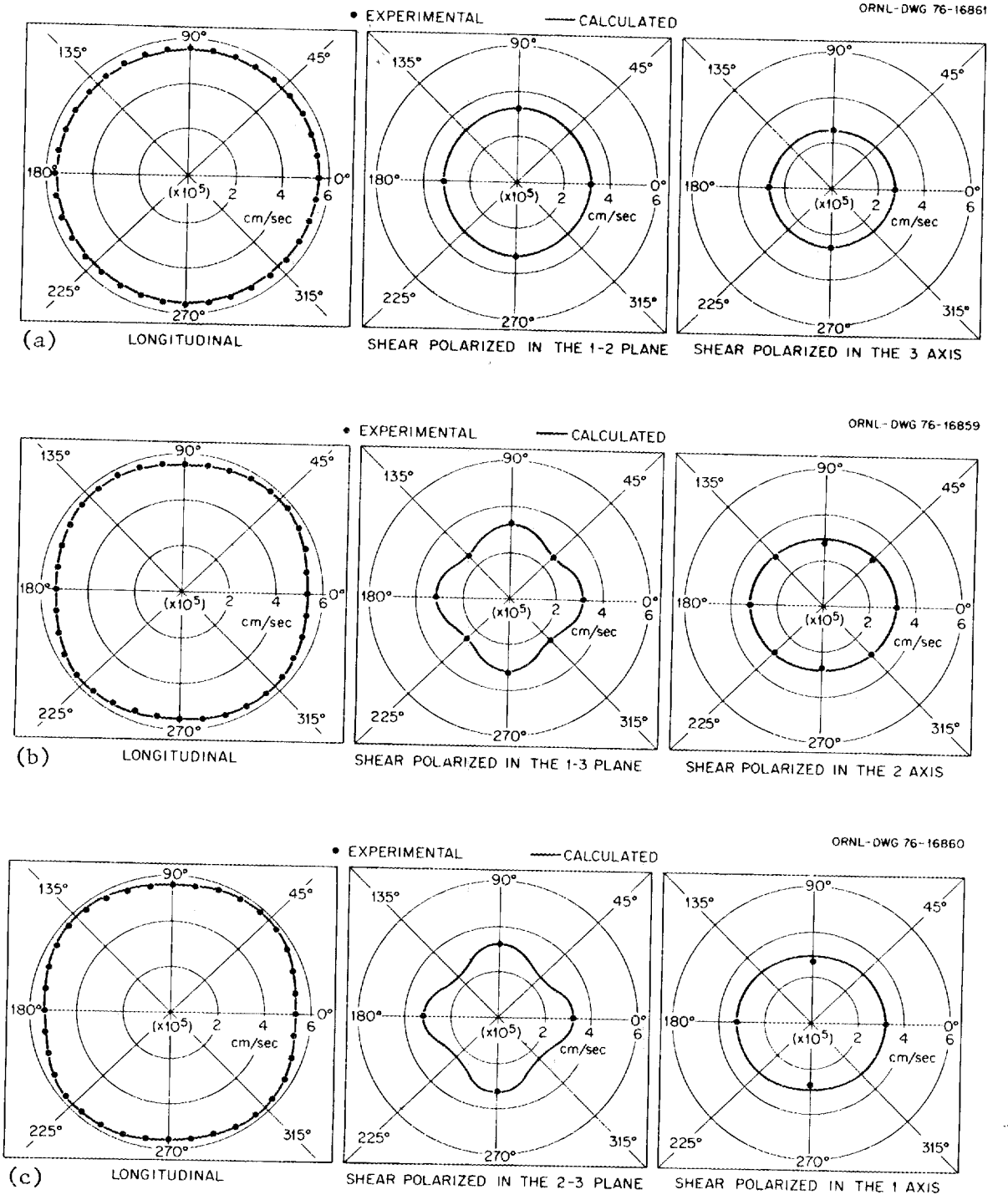

Fig. 6. Variation of Ultrasonic Velocities with Orientation in a Multipass Inconel 82 Weldment. The solid curves are calculated from the Christoffel relation for the assumed orthotropic symmetry. Points are experimental. (a) In 1–2 plane. (b) In the 1–3 plane. (c) In the 2–3 plane.

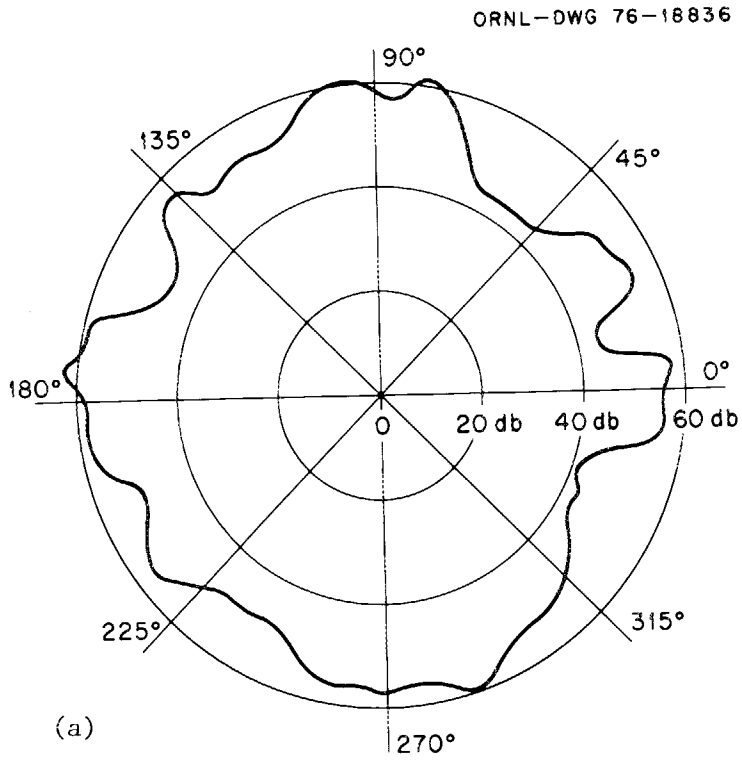

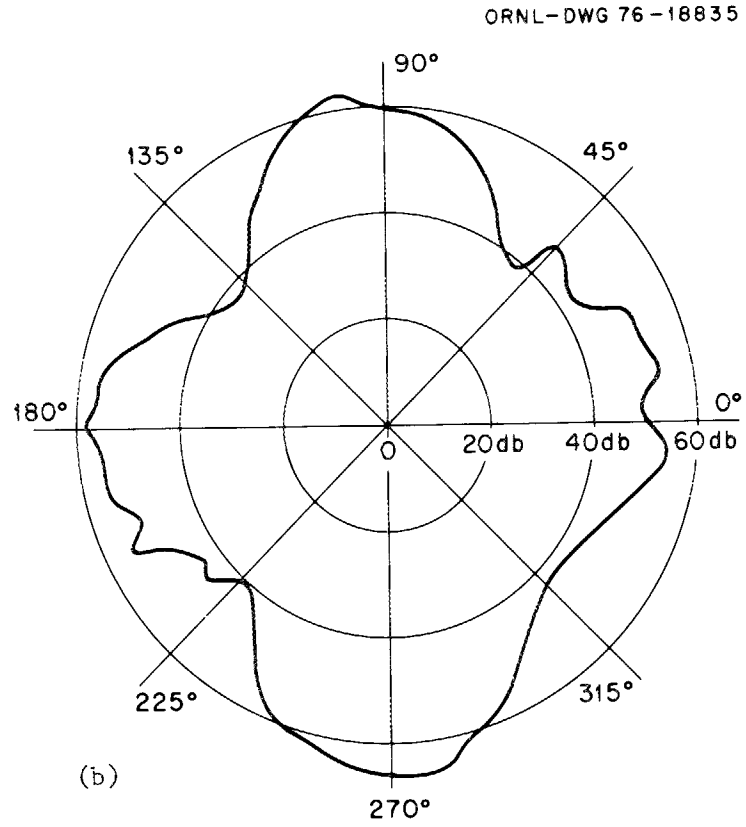

Fig. 7. Variation of Relative Ultrasonic Longitudinal Wave Attenuation with Orientation in a "Single-Pass" Stainless Steel Weld. (a) In the 1–3 plane. (b) In the 2–3 plane.

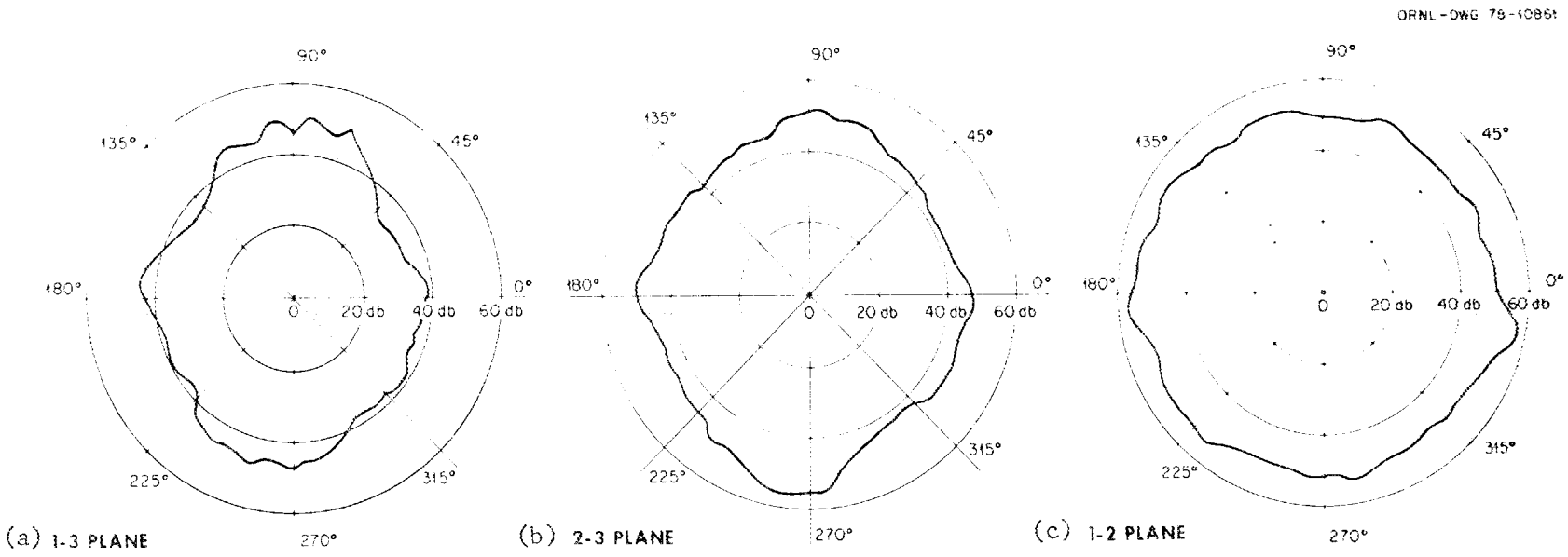

Fig. 8. Variation of Relative Ultrasonic Longitudinal Wave Attenuation with Orientation in a "Multi-Pass" I-82 Weld. (a) In the 1—3 plane. (b) In the 2—3 plane. (c) In the 1—2 plane.

APPARATUS FOR FREQUENCY ANALYSIS

For Analog Data

Figure 9 shows the block diagram of the electronic configuration for ultrasonic frequency analysis. Note that provision has been made for both single transducer pulse-echo and multiple transducer pitch-catch studies. For simplicity all components are synchronized to the ultrasonic pulser. The exciting energy is provided by a high-voltage untuned spike of short duration. For highly damped ceramic or lithium sulfate transducers, the emitted energy covers a relatively broad band of frequencies under these conditions of excitation. The transducer output consists of all received echoes, and for the single transducer, the exciting pulse; these echoes apply to the input of a preamplifier. Recovery of the "preamp" occurs in time to amplify all subsequent echoes, provided a water column of 13 mm or more is used. The output of the preamplifier is fed through the main amplifier to a pedestal-free gate and oscilloscope. The oscilloscope is a monitor to detect distortion in gate input. The delay of the gate adjusts in time, so that any desired segment of the main amplifier radio frequency output may be gated to the spectrum analyzer. The output of the gate consists of two signals: (1) the input waveform plus the gate pulse and (2) the gated portion of the input signal. The latter can be adjusted both in position (time) and in width. Both outputs are displayed simultaneously on a dual-trace oscilloscope and the gated signal is then fed to the spectrum analyzer. The displayed spectrum may then be photographed or recorded on an external device such as an x-y recorder.

Modified Experimental System and Signal Processing

The volume of data from our frequency analyses has become increasingly troublesome to process; therefore, we have redesigned the system to permit computer processing. Figure 10 shows the modified system. The microprocessor controls the analog-to-digital converter and

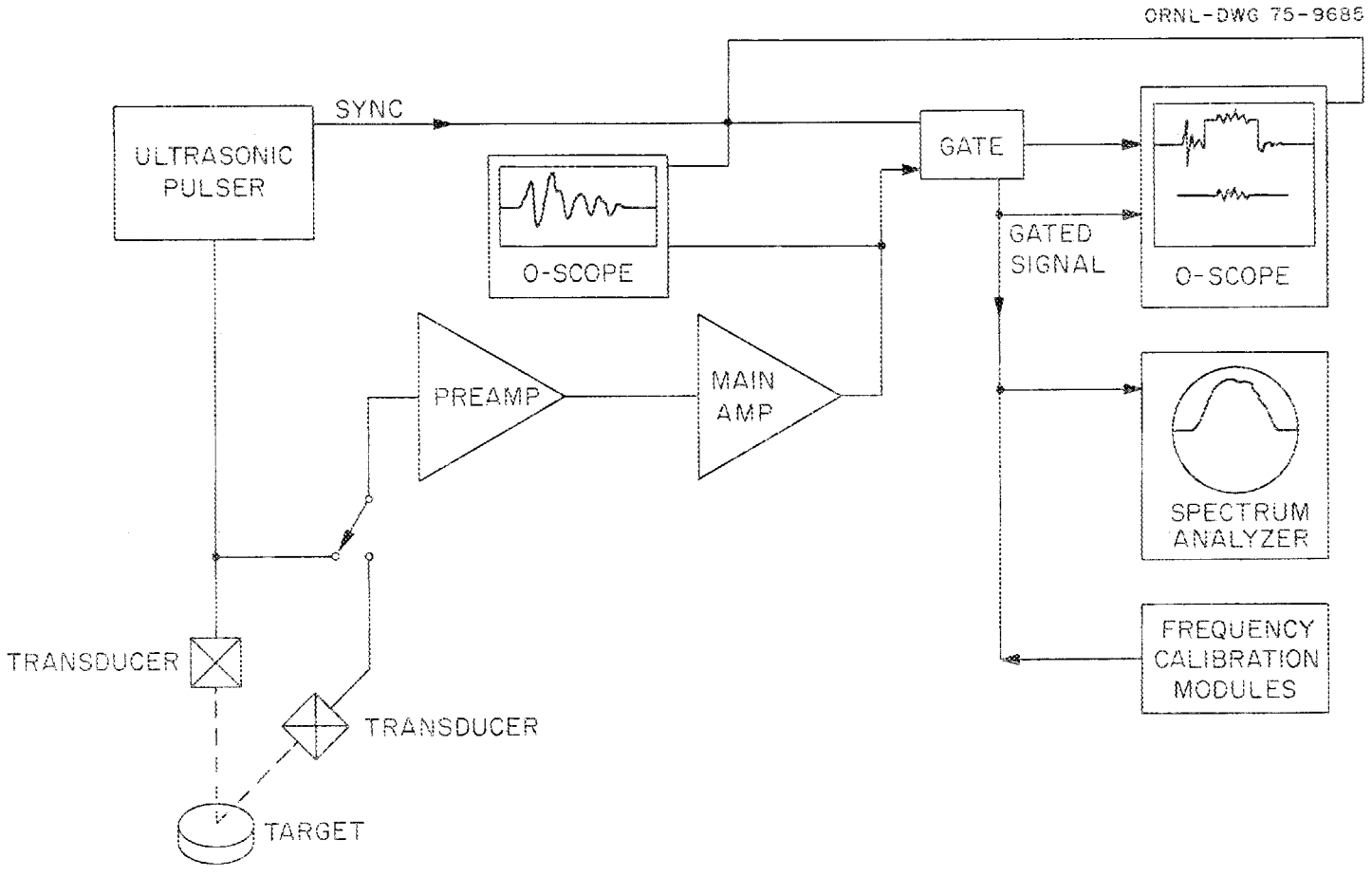

Fig. 9. Analog System for Ultrasonic Frequency Analysis.

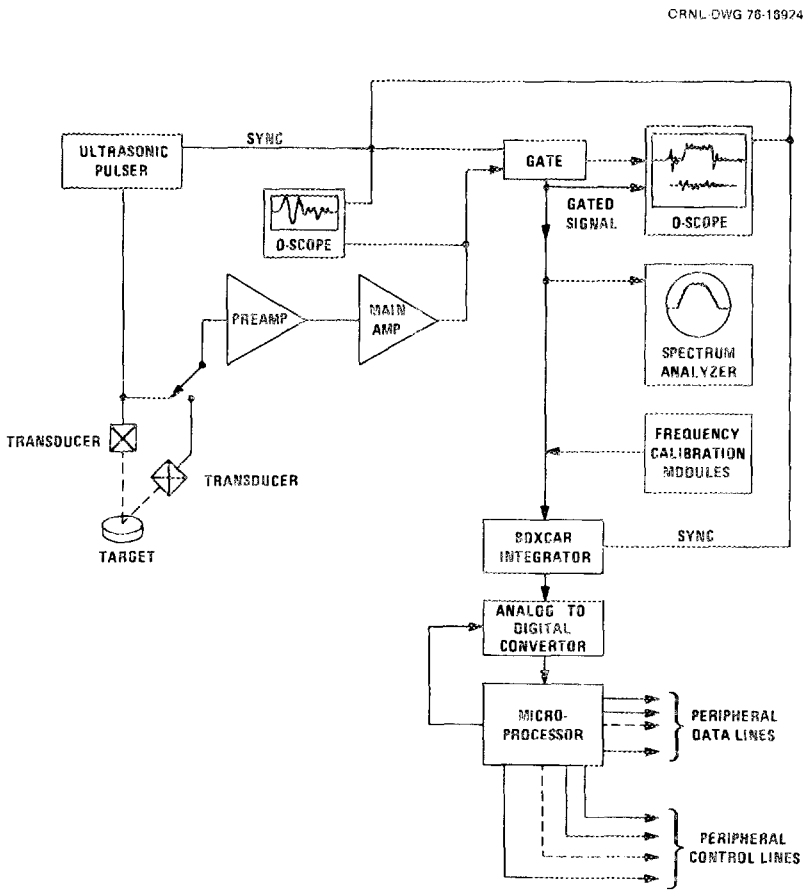

Fig. 10. Block Diagram of the Modified Frequency Analysis System.

converts the binary data to a code format compatible with our peripheral devices. Programs were written to allow the data to be punched on paper tape, displayed on a cathode ray tube terminal, or stored on magnetic tape. Magnetic tapes are preferred for their high-density data-storage capability. The time-series data from magnetic tape are processed by an IBM 360-91 computer using a Fast Fourier Transform program. Another new feature of the modified system is the boxcar integrator. This unit provides a low-frequency facsimile of the ultrasonic waveform and permits the signal to be digitized at a rate far more effective than rates from devices that acquire the waveform directly. Figure 11a shows the waveform of a 40° shear wave scattered by an elliptical flaw with a major axis of 0.8 mm in wrought material. The signal-to-noise ratio in this case is only about three, and if digitized directly, the spectrum

Y-143366

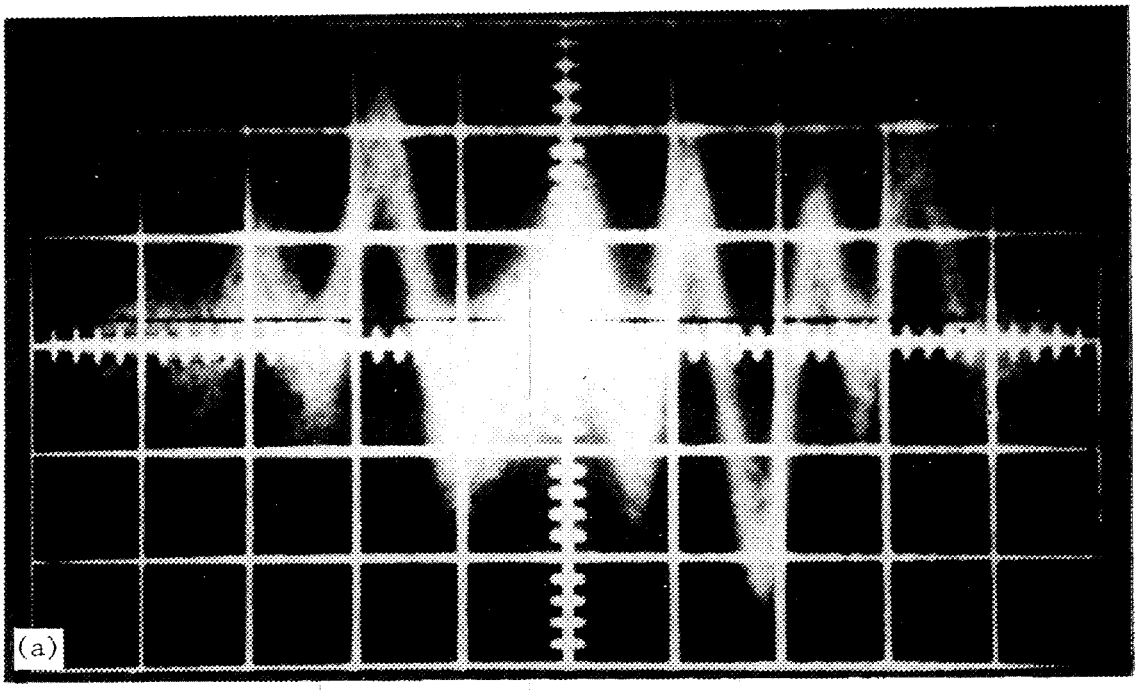

Y-143367

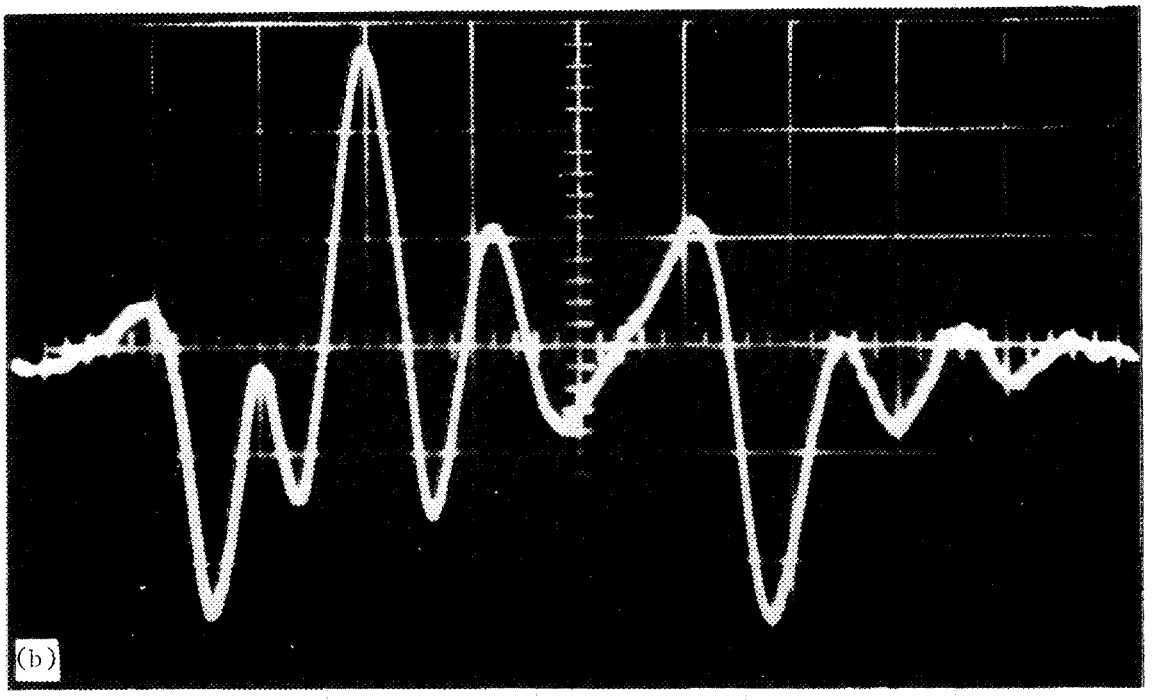

Fig. 11. Signal Obtained from a 0.8-mm Flaw in Metal. (a) Before processing. (b) After processing.

computed from such a signal would be meaningless. Figure 11b shows the signal reconstructed by the boxcar-integrator system. Note the vast signal-to-noise ratio improvement over that of Fig. 11a. The spectrum shown in Fig. 12 was computed from the signal depicted in Fig. 11b. Another advantage of the new system is that it provides both power spectra and the phase of the processed signal. An analog spectrum analyzer furnishes only the power spectra.

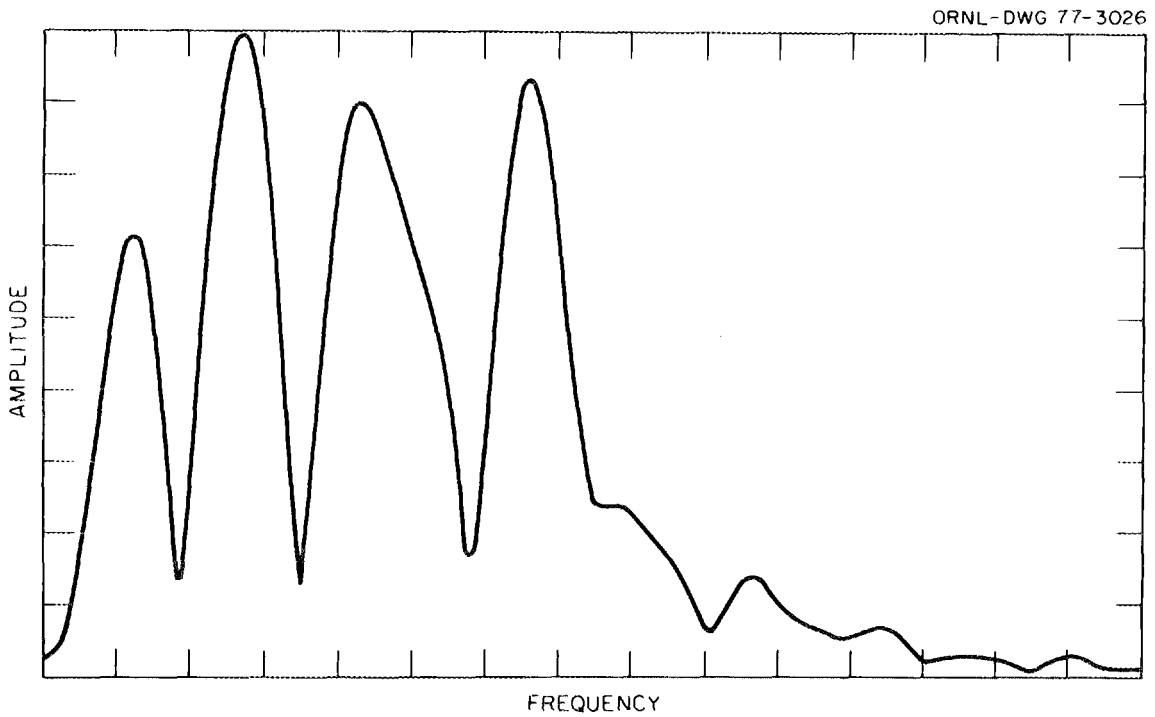

Fig. 12. Spectrum of the Signal Shown in Fig. 11b from an Elliptical Flaw with a Major Axis of 0.8 mm.

RESULTS

Initial experimental work was carried out to characterize defects in 308 weld material. A 6.3-mm-diam. flat-bottomed hole was drilled in the weld. The end of the hole, simulating a circular flaw in the weld, lay in the 1—2 plane, the plane of isotropy. A normally incident

longitudinal wave incident to the plane normal to the defect interacts with the flaw and the diffracted wave emerges at an angle θ. Previous characterization of the weld has defined the functional relationship of ultrasonic velocity to the angle θ (see, for example, Fig. 5).

From the experimental geometry — in our case, normal incidence and a diffracted angle θ — and from Eq. (7) one may calculate the amplitude spectrum. The changes in velocity expected as a change of angle result from the anisotropic behavior of the weld and enter into Eq. (7) as changes in the value of wave number (k).

Plots of experimental and theoretical diffracted amplitude for angles of 15 and 36° are presented in Figs. 13 and 14. Figure 15 illustrates the experimentally determined spectrum for a diffracted shear wave at an angle of 30°.

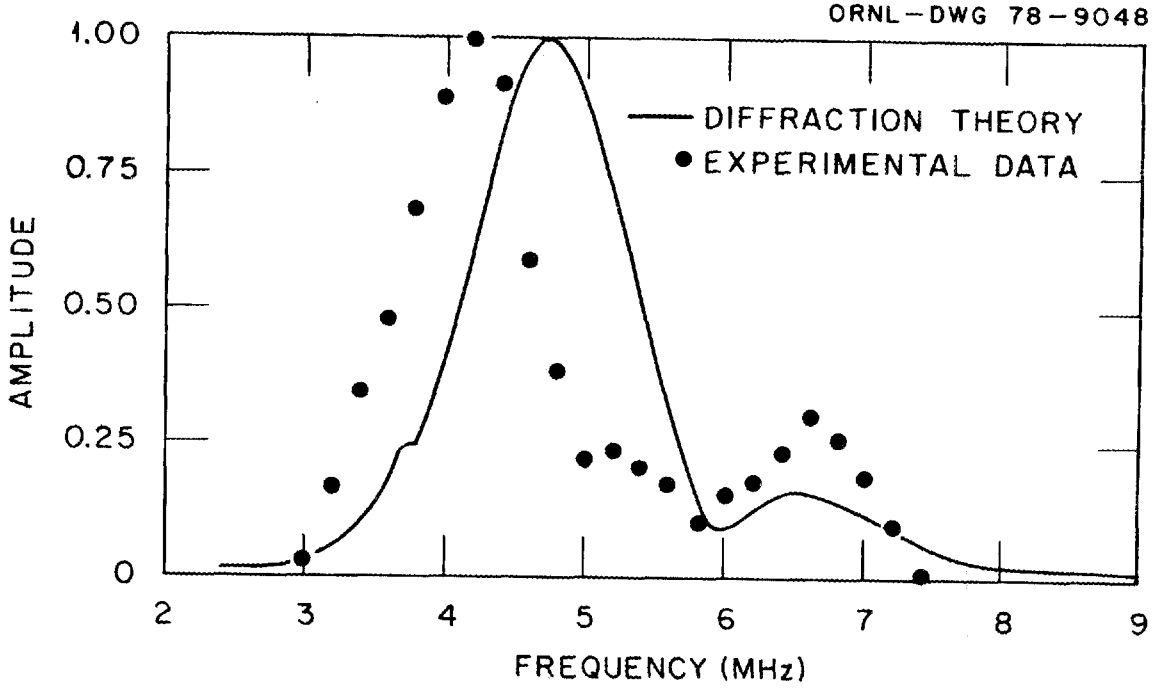

Fig. 13. Spectra of Longitudinal Waves Diffracted at $\theta = 15°$ from a 6.3-mm Flat-Bottomed Hole. The solid line denotes the theoretical spectrum. Points are experimental.

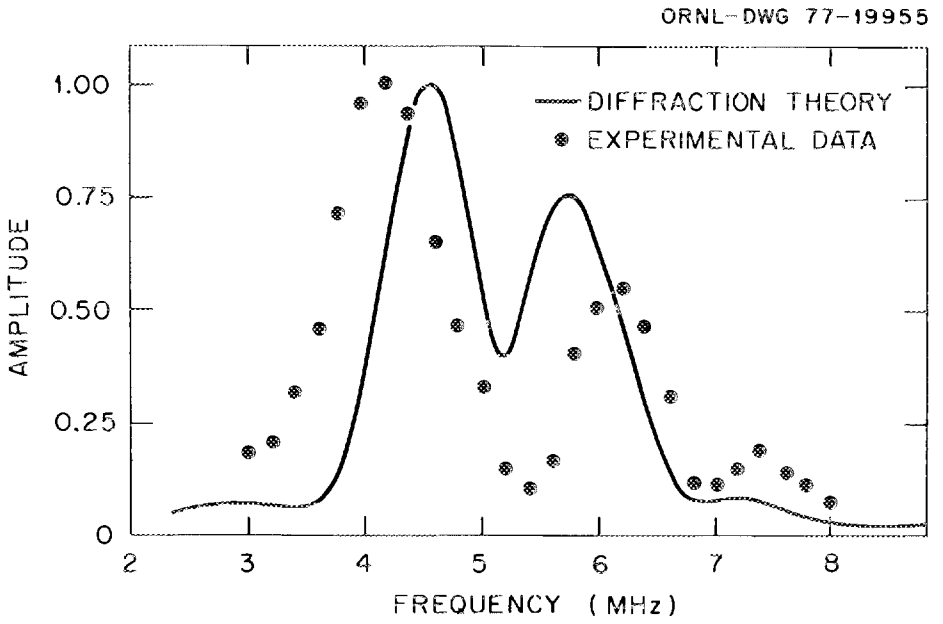

Fig. 14. Spectra of Longitudinal Waves Diffracted at $\theta = 36°$ from a 6.3-mm Flat-Bottomed Hole. The solid line denotes the theoretical spectrum. Points are experimental.

Y-152660

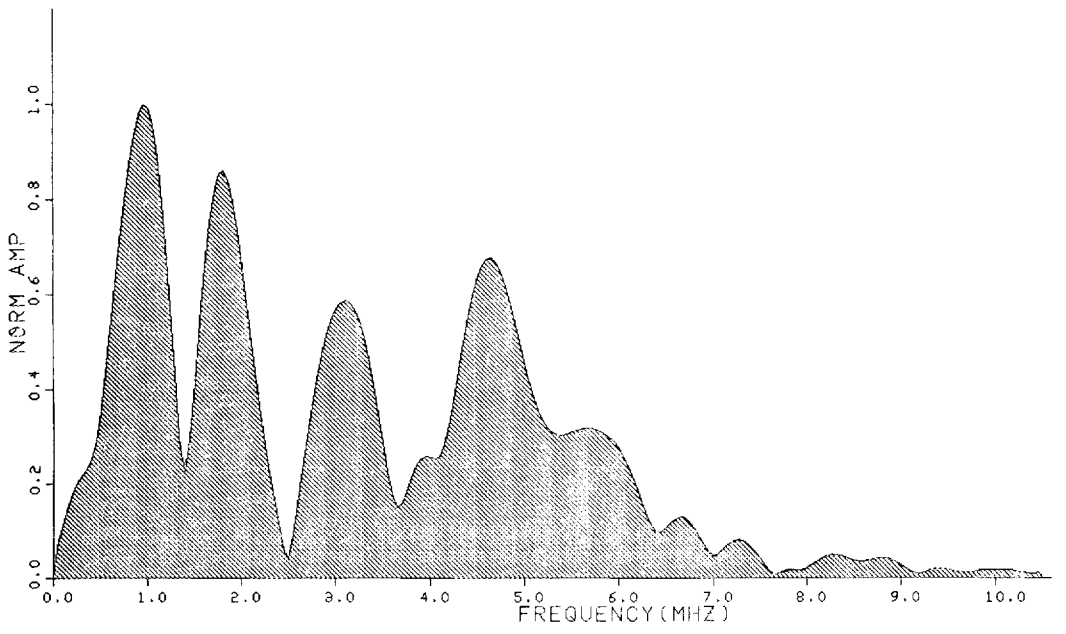

Fig. 15. Experimentally Determined Spectrum of Shear Waves Diffracted from a 6.3-mm Flat-Bottomed Hole.

Figure 16 demonstrates the error that could be made in predicting the amplitude spectra if mechanical isotropy were assumed when the material was actually anisotropic. The spectrum for the highest velocity shown is the true diffracted amplitude distribution when anisotropy is accounted for; that is, it is the distribution that would be measured. The spectrum in the foreground of the plot is that predicted when isotropy is assumed. The figure dramatically demonstrates the absolute necessity of correcting for velocity variation within the weld. The greatest error results from a 45° diffracted shear wave, because of the large variations in velocity with orientation. Ironically, 45° is the most commonly used angle for testing welds. Both size and location of a weld defect can be misjudged by as much as 40% unless the procedure we have described is followed.

ORNL-DWG 77-3300

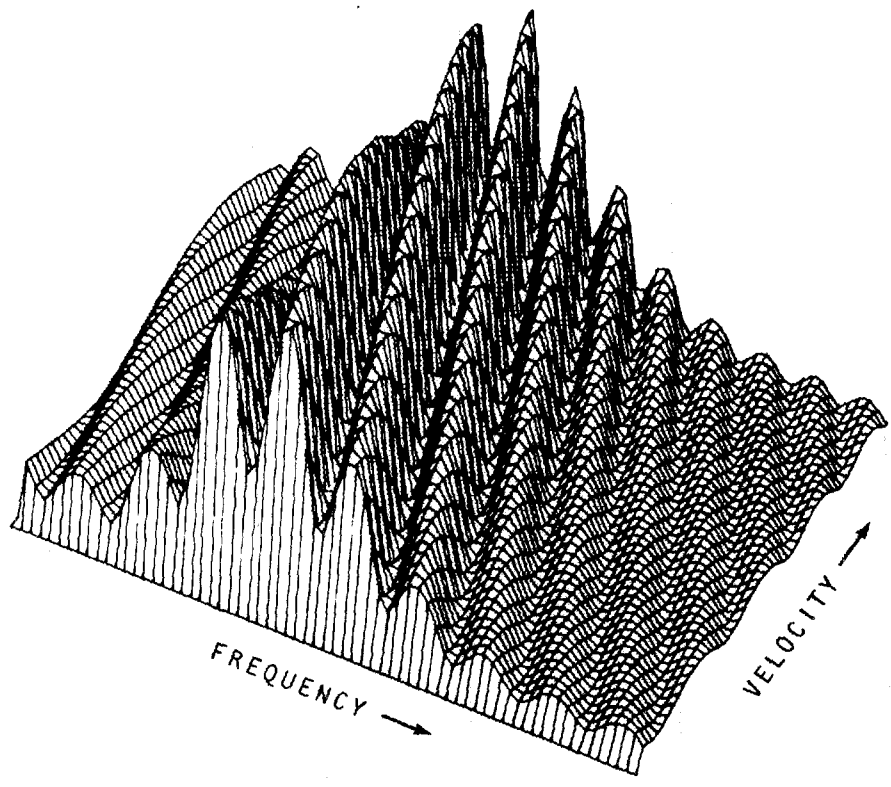

Fig. 16. Effect of Anisotropy on the Amplitude Spectrum of a 45° Diffracted Shear Wave in Stainless Steel Weld Metal.

ACKNOWLEDGMENTS

The authors wish to thank R. W. McClung for suggestions and advice. Thanks are also due to H. T. Murrin and R. A. Cunningham for their many contributions — especially their construction of the accurate mechanical fixtures. We would also like to thank Nancy Richards for editing, and Jan Renfro for typing this manuscript.

REFERENCES

1. H. L. Whaley and L. Adler, "Flaw Characterization by Ultrasonic Frequency Analysis," *Mater. Eval.* 29: 182–92 (1971).
2. B. R. Dewey, L. Adler, R. T. King, and K. V. Cook, "Measurement of Anisotropic Elastic Constants for Type 308 Stainless Steel Electroslag Weld," *Exp. Mech.* 17(11): 420–26 (1977).
3. L. Adler and H. L. Whaley, "Interference Effect in a Multifrequency Ultrasonic Pulse Echo and Its Application to Flaw Characterization," *J. Acoust. Soc. Am.* 51(3): 881–87 (1972).
4. H. L. Whaley, K. V. Cook, L. Adler, and R. W. McClung, "Applications of Frequency Analysis in Ultrasonic Testing," *Mater. Eval.* 33(1): 19–24 (January 1975).
5. W. A. Simpson, "Time-Frequency Domain Formulation of Ultrasonic Frequency Analysis," *J. Acoust. Soc. Am.* 56: 1776–81 (December 1974).
6. L. Adler and D. K. Lewis, "Diffraction Model for Ultrasonic Frequency Analysis and Flaw Characterization," *Mater. Eval.* 35(1): 51–56 (January 1977).
7. L. Adler, K. V. Cook, H. L. Whaley, and R. W. McClung, "Flaw-Size Measurement in a Weld Sample by Ultrasonic Frequency Analysis," *Mater. Eval.* 35(3): 44–50 (March 1977).
8. J. B. Keller, "Diffraction by an Aperture," *J. Appl. Phys.* 28(4), 426–44 (April 1957).

ORNL/TM-6456
Distribution
Category
UC-79b, -h, -k

INTERNAL DISTRIBUTION

1–2. Central Research Library
3. Document Reference Section
4–6. Laboratory Records Department
7. Laboratory Records, ORNL RC
8. ORNL Patent Office
9–13. L. Adler
14–18. K. V. Cook
19. J. M. Corum
20–24. J. R. DiStefano
25. D. W. Fitting
26–28. M. R. Hill
29. K. C. Liu
30–54. R. W. McClung
55. H. E. McCoy, Jr.
56. C. E. Pugh
57. W. A. Simpson
58. G. M. Slaughter
59. J. H. Smith
60. R. W. Balluffi (consultant)
61. P. M. Brister (consultant)
62. W. R. Hibbard, Jr. (consultant)
63. M. J. Mayfield (consultant)
64. N. E. Promisel (consultant)
65. J. Stringer (consultant)

EXTERNAL DISTRIBUTION

66–67. DOE DIVISION OF REACTOR RESEARCH AND TECHNOLOGY, Washington, DC 20545

Director

68–69. DOE OAK RIDGE OPERATIONS OFFICE, P.O. Box E, Oak Ridge, TN 37830

Director, Research and Technical Support Division
Director, Reactor Division

70–335. DOE TECHNICAL INFORMATION CENTER, Office of Information Services, P.O. Box 62, Oak Ridge, TN 37830

For distribution as shown in TID-4500 Distribution Category, UC-79b (Fuels and Materials Engineering Development); UC-79h (Structural Materials Design Engineering); and UC-79k (Components).